ORIGINAL PAPER

Simultaneous voltammetric determination of ascorbic acid and dopamine at the surface of electrodes modified with self-assembled gold nanoparticle films

Jahan Bakhsh Raoof · Abolfazl Kiani · Reza Ojani · Roudabeh Valiollahi · Sahar Rashid-Nadimi

Abstract Gold nanoparticles (GNs) could be efficiently immobilized on binary mixed self-assembled monolayers (SAMs) on a gold surface composed of 1,6-hexanedithiol and 1-octanethiol (nano-Au/SAMs gold electrode). This GN chemically modified electrode was used for electrochemical determination of ascorbic acid (AA) and dopamine (DA) in aqueous media. The result showed that the GN-modified electrode could clearly resolve the oxidation peaks of AA and DA, with a peak-to-peak separation (ΔE_p) of 110 mV enabling determination of AA and DA in the presence of each other. The linear analytical curves were obtained in the ranges of 0.3–1.4 mM for AA and 0.2–1.2 mM for DA concentrations using differential pulse voltammetry. The detection limits (3σ) were 9.0×10^{-5} M for AA and 9.0×10^{-5} M for DA.

Introduction

The design of new nanoscale materials has acquired ever greater importance in recent years due to their wide-ranging applications in various fields. Among these materials, metallic nanoparticles are of great interest due to their important properties and their numerous possible applications [1, 2]. The metal nanoparticles have size-dependent unique chemical, electrical, and optical properties and are very promising for practical applications in diverse fields such as multifunctional reagent and biosensors [3–9]. The nanoparticles are very different from bulk materials and their electronic, optical, and catalytic properties originate from their quantum scale dimensions (<2 nm) [10]. The electrocatalytic activity of metal nanoparticles is strongly dependent on their composition, size, surface area, and surface morphology [11]. Noble metal nanoparticles have been extensively utilized in recent years, owing to their extraordinarily catalytic activities for both oxidation and reduction reactions. To obtain high surface area, metal nanoparticle catalysts were usually dispersed in an organic polymer such as nafion [12, 13], colloids [14], surfactants [15], and porous substrates, which enable metal particles to be highly dispersed and stable.

Due to the unique properties of gold nanoparticles (GNs), such as good conductivity, useful electrocatalytic ability, and biocompatibility, several researchers have been attracted to fabricate electrochemical sensors and biosensors [16–19]. The GNs dispersed on various substrates such as carbon paste electrode; conducting and non-conducting polymers and self-assembled monolayer have been reported. The fabrication of sensors based on self-assembly GNs nanostructure is of recent technological interest [20–23]. Arrays of GNs have been utilized for electrochemical sensors as they exhibit excellent catalytic activity towards various reactions [24]. In these, the GNs function as an "electron antennae", efficiently tunneling electrons between the electrode and electrolyte [25].

J. B. Raoof (✉) · R. Ojani · R. Valiollahi · S. Rashid-Nadimi
Chemistry Research Laboratory,
Department of Analytical Chemistry, Faculty of Chemistry,
Mazandaran University,
Babolsar, Iran
e-mail: j.raoof@umz.ac.ir

A. Kiani
Department of Chemistry, Faculty of Science,
University of Isfahane,
Isfahane, Iran

Dopamine (DA) plays an important physiological role as an extracellular chemical messenger (neurotransmitter (NTM)). Because the loss of NTM may result in some serious diseases, e.g., Parkinson's disease and schizophrenia, the determination of such a component in real biological samples is an obvious target in neurochemical studies [26]. Apart from the need to reach low detection limits, determination of DA is complicated by the coexistence of many interfering compounds. Among them, ascorbic acid (AA) is of particular importance [27]. Ascorbic acid accompanies DA in biological samples: for instance, in the extracellular fluid of central nervous system, AA is present at the 100–500 µM concentration, whereas the concentration of DA is less than 100 nM [28].

Determination of ascorbic acid (AA) by voltammetric methods has received much attention in recent years [29]. It has been shown that content of AA in biological fluids can be used to access the amount of oxidation stress in human metabolism and excessive oxidative stress has been linked to cancer, diabetes and hepatic disease [30]. It is known that accurate determination of AA using conventional electrodes is very difficult because of its high overpotential, poor reproducibility due to fouling effect caused by the oxidized products of AA, low selectivity, and low sensitivity. Thus, development of new methods for determination of AA and DA in same sample has received considerable interest in recent years. Wang et al. reported fabrication of layer-by-layer modified multilayer films containing choline and gold nanoparticles and its sensing application for electrochemical determination of dopamine and uric acid [31]. Voltammetric peak separation of dopamine from uric acid in the presence of ascorbic acid is performed based on hot-wire voltammetry which needs an increase in temperature of the working electrode [32]. Recently, conducting polymer-based selective detection of dopamine in the presence of ascorbic acid and uric acid was reported [33]. To the best of our knowledge, there is no published report on simultaneous determination of dopamine and ascorbic acid at the surface of gold nanoparticles although ruthenium oxide-modified electrode is applied for this purpose [34].

Our group was interested in the development of an electrochemical sensor for the detection of different biomolecules [35–37]. In an effort to develop a method for the determination of ascorbic acid (AA) and dopamine (DA), we report the fabrication of gold nanoparticle-modified gold electrode based on the self-assembly of gold nanoparticles at the surface of mixed film of 1,6-hexanedithiol (HDT) and 1-octanethiol (OT) which is self-assembled at gold electrode. Free —SH group of HDT was used as a scaffold to immobilize GNs. The film formed by this technique has the advantages of high organization and uniformity, which could provide a desirable microenvironment for the assembly of GNs. Cyclic voltammetric, and differential pulse voltammetric methods were used for the characterization of the gold nanoparticle-modified electrodes (GNMEs) and its electrocatalytic activity toward the ascorbic acid and dopamine oxidations. The modified electrode showed good stability and can be applied for selective determination of ascorbic acid and dopamine in the presence of each other.

Experimental

Chemicals

1,6-Hexanedithiol (HDT), 1-octanethiol (OT), ascorbic acid (AA), dopamine (DA) (from Fluka), tetrachloroauric(III) acid trihydrate (HAuCl$_4$·3H$_2$O), potassium hexacyanoferrate (II), and potassium chloride were purchased from Merck. Potassium chloride was used as the supporting electrolyte. Buffer solutions were prepared from ortho-
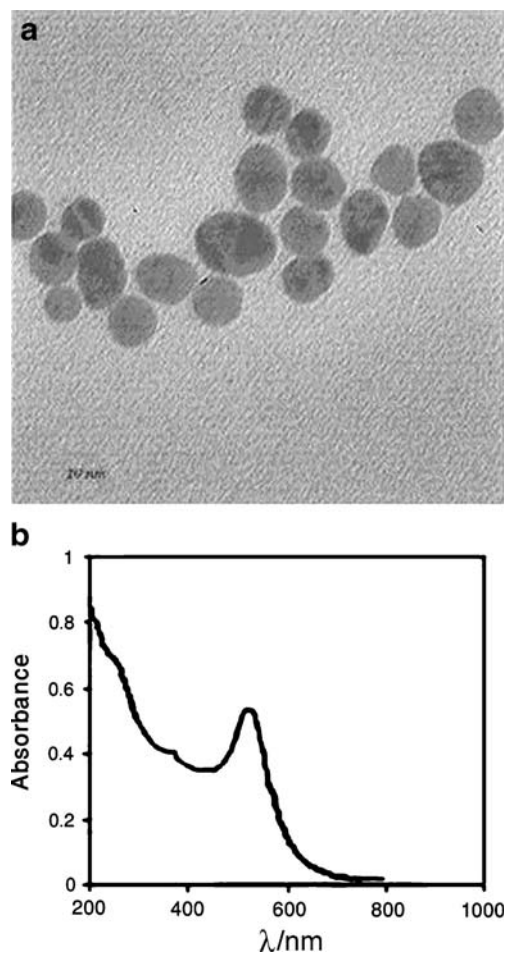
Fig. 1 a TEM micrograph of the as-prepared gold nanoparticles. Specimens were prepared by evaporating a drop of aqueous solution containing gold nanoparticles onto a copper mesh grid. **b** UV–visible spectra of colloidal gold nanoparticles

phosphoric acid and its salts in the pH ranges of 2.00–7.00. Freshly prepared solution of DA and AA were used in all experiments. Twice-distilled water was used to preparation of buffered and reagent solutions.

Preparation of Au nanoparticles

The colloidal gold solutions were prepared according to the method reported elsewhere [38]. Briefly, in a round-bottom flask, 100 mL of 0.01% $HAuCl_4$ solution was brought to boiling with vigorous stirring, and then 2.5 mL of 1% sodium citrate solution was quickly added to give a color change from blue to red violet. Boiling continued for an additional 10 min, then the heater was removed and the mixture was stirred continuously for another 10 min. Finally, the cooled Au colloid was stored at 4°C in a dark bottle.

Instrumentation

The electrochemical experiments such as cyclic voltammetry and differential pulse voltammetry (DPV) were carried out using a potentiostat/galvanostat (BHP 2061-C Electrochemical Analysis System, Behpajooh, Iran) coupled with a Pentium IV personal computer. The following optimized parameters were used to record the differential pulse voltammograms: pulse height 50 mV, step width 2 s, and pulse time 50 ms. Electrochemical measurements were performed in a three-electrode cell with a polished Au electrode or GNME as working electrode, a Pt wire as counter electrode, and saturated calomel electrode (SCE) as reference electrode. Thus, all potentials are referenced to the SCE. The size of the GNPs was determined with a LEO-912AB high-resolution transmission electron microscope operating at 120 kV. UV–visible spectra were measured using a double-beam Cecil 5505 UV–visible spectrophotometer with 1.0-cm-path-length cells and photomultiplier tube detector (Cambridge UK).

Cyclic and square-wave (SW) voltammograms were recorded using a computer-controlled BAS 100B/W electrochemical analyzer.

Results and discussion

Characterization of gold nanoparticles

The transmission electron microscopy image indicates that the average size of GNs is 16 nm (Fig. 1a). Figure 1b depicts the UV–visible absorption spectrum of colloidal GNs (λ_{max}=520 nm). It has been shown that n-Au with a diameter of 2.6 nm would give an absorption maximum at around 514 nm, whereas the particles with a diameter of 20–40 nm would exhibit an absorption band between 530 and 540 nm [7, 39].

Electrode pretreatment and modifications

The working electrode was a Au disk electrode with a diameter of 3 mm. Prior to each measurement, the Au working electrode (Metrohm) was polished with alumina slurry down to 0.05 µm on a polishing cloth followed by sonicating in distilled water and absolute ethanol. Then the Au electrode was electrochemically cleaned by cycling the electrode potential between −0.2 and 1.4 V vs. SCE in 0.5 M H_2SO_4 at a scan rate of 100 mV s^{-1} until the cyclic voltammetry characteristics for a clean Au electrode were obtained. Then the clean gold electrode was immersed in absolute ethanol solution containing 1.0 mM of HDT and 20 mM of OT for 20 h. OT serve as diluents during the self-assembly process which is expected to result in better self-assembled monolayers (SAMs). It is because the structure of HDT could make a bridge at Au substrate as bearing two thiol groups. With choosing 1-octanethiol+1,6-dihexanethiol with ratio of 20:1, the probability of bridging for 1,6-dihexanethiol was reduced and it caused the nanogold to be immobilized on the modified surface separately and behave as nanoelectrode arrays.

Upon removal from the deposition solution, the substrate was thoroughly rinsed with ethanol and water to remove the physically adsorbed HDT and OT from the electrode surface and then dipped into Au colloidal solution for

Scheme 1 Schematic representation of **a** formation of HDT+OT monolayer on Au and **b** immobilization of GNs on HDT+OT-modified Au electrode in pH5.0
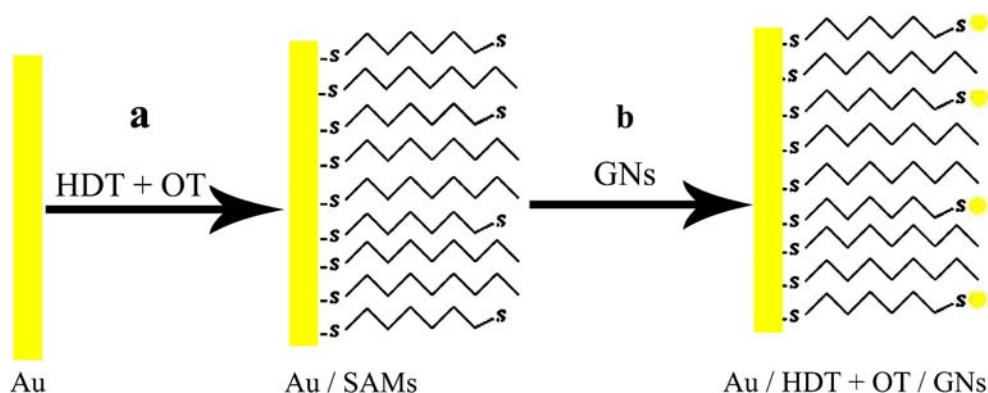
3.5 h. Immobilization of GNs on polycrystalline Au electrode is typically shown in Scheme 1. The resultant electrode was washed with water and used for electrochemical measurements.
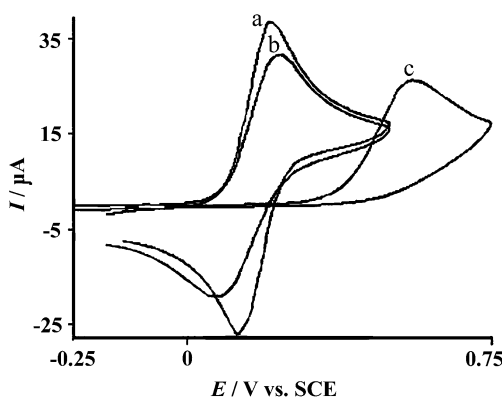
Characterization of nano-Au electrode with cyclic voltammetry

Cyclic voltammetry of redox system $[Fe(CN)_6]^{4-}$ is a valuable tool for testing the kinetic of the barrier of the interface because the extent of kinetic hindrance to the electron transfer process increases with the increasing thickness and the decreasing defect density of the barrier. Figure 2 shows the CV responses of 2.0 mM $[Fe(CN)_6]^{4-}$ at bare Au, HDT/OT/Au, and GNME, respectively. As can be seen, $[Fe(CN)_6]^{4-}$ shows a couple of well-defined redox wave at bare Au (Fig. 2, curve a) with a peak-to-peak separation (ΔE_p) of 75 mV at 100 mV s^{-1}, which is larger than expected for a one electron transfer reversible reaction. After modifying the electrode with HDT/OT SAMs, an obvious decrease in redox peak current is observed (Fig. 2, curve b), indicating that the HDT/1-octanethiol SAM act as the barrier to electron transfer and mass transfer blocking layer and thus hinders the diffusion of ferrocyanide toward the electrode surface. On the contrary, when GNs was attached to electrode surface, the voltammetric response of ferrocyanide is restored similar to that obtained at the bare Au (Fig. 2, curve c).
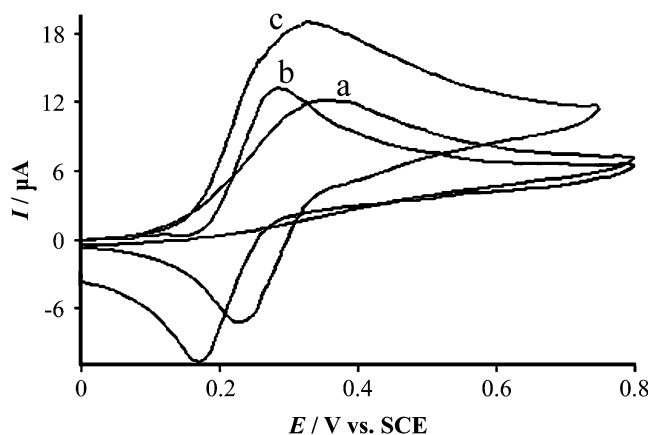
This demonstrated that GNs has been successfully assembled on Au surface and provide the necessary condition pathways, besides acting like nanoscale electrodes in electron transfer between the analyte and the electrode surface.

The electrochemical response of AA and DA at the GNME

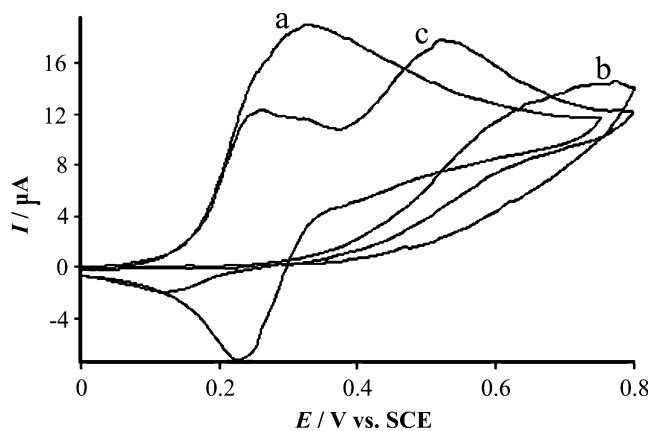We have utilized GN-modified electrode for the determination of ascorbic acid and dopamine. Figure 3 shows

Fig. 3 Cyclic voltammograms of **a** 1.0 mM AA, **b** 1.0 mM DA, **c** mixture of 1.0 mM AA and 1.0 mM at bare Au in 0.1 M phosphate buffer+0.1 M KCl at pH5.00. Potential scan rate was 20 mV s^{-1}

the cyclic voltammograms obtained for AA (curve a), DA (curve b), and a solution of AA and DA in the presence of each other (curve c) in 0.1 M phosphate buffer solution (pH=5.00) at bare Au electrode. The irreversible oxidation of AA occurs at 360 mV vs. SCE at bare Au electrode (Fig. 3, curve a). Figure 3c shows the electrooxidation of AA and DA at same potential and bare Au electrode cannot resolve the oxidation peaks of AA and DA. The oxidation of AA can be catalyzed with oxidized form of DA, because the cathodic current of DA was decreased in the presence of AA and its anodic current was increased (comparison of curves a and c of Fig. 3).

Figure 4 shows the cyclic voltammograms of 1.0 mM AA and 1.0 mM DA in 0.1 M phosphate buffer solution (pH=5.00) at the surface of Au, Au-HDT/OT SAM electrodes, and GNME. As can be seen, both bare Au and Au-HDT/OT SAM electrodes fail to separate the oxidation peaks of AA and DA (Fig. 4, curves a and b). However,

Fig. 2 Cyclic voltammograms of 2.0 mM $[Fe(CN)_6]^{4-}$ in 0.1 M KCl at **a** bare Au, **b** HDT/OT/Au electrode, and **c** GNME. Potential scan rate was 100 mV s^{-1}

Fig. 4 Cyclic voltammograms obtained for 1.0 mM AA+1.0 mM DA at **a** bare Au, **b** Au/HDT/OT electrode, and **c** GNME in 0.1 M phosphate buffer+0.1 M KCl at pH5.00. Potential scan rate was 100 mV s^{-1}

| pH	3.00	4.00	5.00	6.00	7.00
ΔE_p (mV)	0.0	196	280	0.0	0.0

GNME electrode resolves the oxidation peaks of AA and DA, where oxidation of AA occurs at 250 mV while the oxidation of DA occurs at 530 mV vs. SCE (Fig. 4, curve c). Also, the comparison of AA electrooxidation at the surface of bare Au electrode (Fig. 3, curve a) and GNME (Fig. 4, curve c) show that the electrooxidation peak potential of AA at GNME is shifted about 110 mV to less positive potential due to the high catalytic activity of Au nanoparticle.

On the contrary of bare Au electrode, 1,6-hexanethiol (HDT) with pK_a=10.24 (http://www.chemicalbook.com) presents as protonated form in pH=5.00 which is positively charged, while citrate ions as stabilizer give negative charge to GNs. Therefore, the resultant charge seems to be a positive charge that is opposite with the charge of AA form in this pH (AA—pK_{a1}=4.17 and

pK_{a2}=11.8) (http://www.chemicalbook.com). Also, probably the negatively charges of AA form in this pH can be replaced with citrate ions for stabilization of GNs. Therefore, the electrooxidation of AA at the surface of this modified electrode shifted to less positive potential. As can be seen in Fig. 4, the electrooxidation of DA at the surface of this modified electrode was moved to more positive potential because of the electrochemical repulsion of positive charge between the DA and the surface of this electrode. Also, similar to our result, Ohsaka et al. employed gold nanoparticles immobilized on an amine-terminated self-assembled monolayer on a polycrystalline Au electrode successfully for the selective determination of DA in the presence of AA [40]. Therefore, well-separated voltammetric peaks were observed for DA and AA at the GNME.

Influence of pH on GNME response

The value of the separation in voltammetric peak potential of AA and DA is influenced by pH of solution. Cyclic voltammetry was carried out for the study of solution pH on electrochemical behavior of AA and DA at the GNME. The
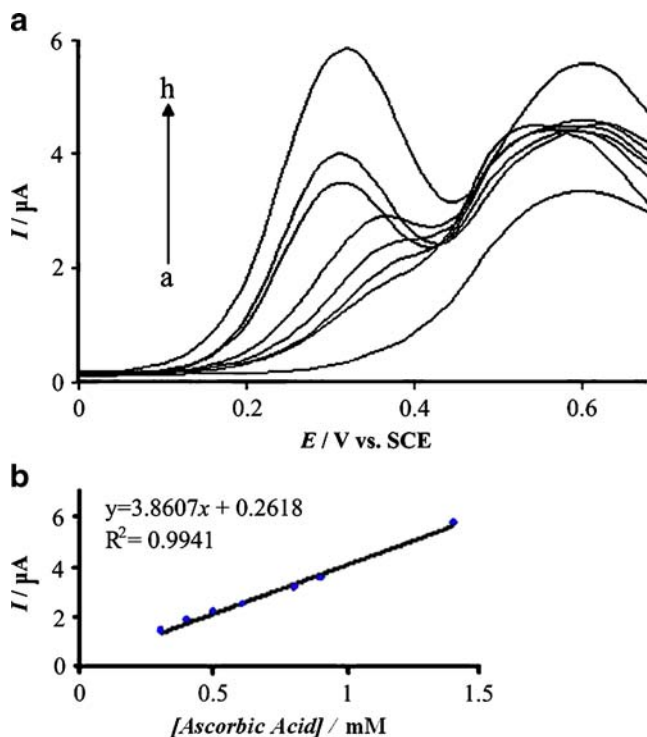
Fig. 5 a Differential pulse voltammograms of AA at various concentration: (1) 0.00 mM; (2) 0.30 mM; (3) 0.40 mM; (4) 0.50 mM; (5) 0.60 mM; (6) 0.80 mM; (7) 0.90 mM; and (8) 1.4 mM in the presence of 1.0 mM DA in 0.1 M phosphate buffer+ 0.1 M KCl (*pH*=5.00) at GNME at potential scan rate 20 mV s^{-1}. **b** The plot of oxidation peak currents vs. AA concentrations derived from voltammograms of (**a**)
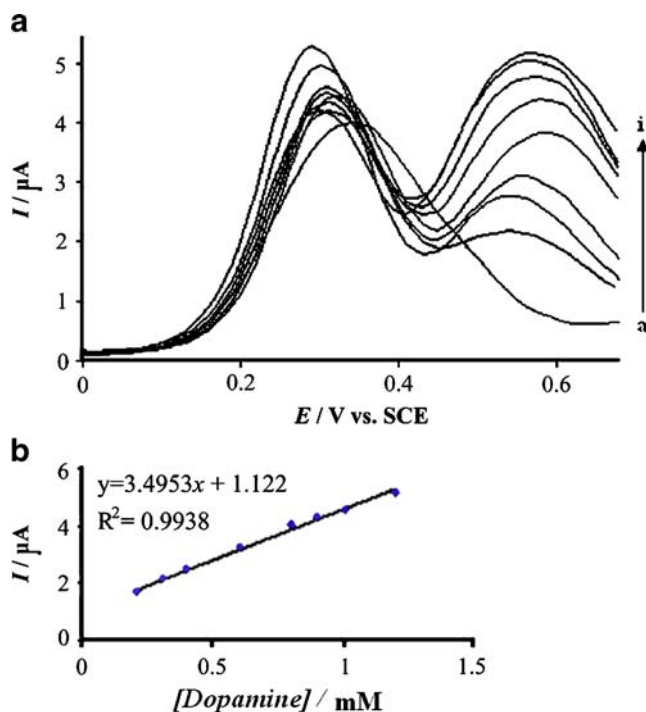
Fig. 6 a Differential pulse voltammograms of DA obtained at various concentrations: (1) 0.00 mM; (2) 0.20 mM; (3) 0.30 mM; (4) 0.40 mM; (5) 0.60 mM; (6) 0.80 mM; (7) 0.90 mM; (8) 1.00 mM; and (9) 1.2 mM in the presence of 1.0 mM AA in 0.1 M phosphate buffer+0.1 M KCl (pH=5.00) at GNME at scan rate 20 mV s^{-1}. **b** The plot of oxidation peak currents vs. DA concentrations derived from voltammograms of (**a**)

oxidation peak potentials of both DA and AA were shifted to less positive values with increasing pH. This is a consequence of a deprotonation step involved in both oxidation processes that is facilitated at higher pH [41–43]. The anodic peak potential difference increased with the increase in pH from pH 3.00 to pH 5.00 and then decreased (Table 1).

Based on obtained results, to obtain a maximum peak separation for anodic oxidation of AA and DA, the pH was adjusted to 5.00. The observed 280 mV peak separation is more than enough to determine the concentration of both AA and DA simultaneously in a mixture. Therefore, the best separation in anodic peak potentials for simultaneous voltammetric determination of AA and DA was obtained in pH 5.00.

Analytical performance of GNME for simultaneous determination of DA and AA

The electrooxidation peak currents of AA and DA at the surface of the GNME can be used for determination of these compounds in solution. Therefore, DPV experiment was performed using GNME in phosphate buffer solution containing various concentrations of each compound. The analytical experiments were carried out either by varying the AA concentration in the presence of fixed 1.0 mM DA or by varying the concentration of DA in the presence of fixed 1.0 mM AA in buffer solution at GNME (pH=5.00). Figure 5a shows the differential pulse voltammograms of increasing concentrations of AA in the presence of 1.0 mM DA at GNME. The analytical plot (Fig. 5b) for voltammetric determination of AA is linear in the range of 0.30–1.40 mM of AA concentration with a correlation coefficient (R^2) of 0.9941 ($n=7$). The detection limit (3σ) was 9.0×10^{-5} M.

The electrooxidation of DA in different concentrations was investigated in the presence of fixed concentration of AA in phosphate buffer medium (pH=5.00) at the surface of GNME using DPV method. Typical differential pulse voltammograms are shown in Fig. 6a. The analytical curve (Fig. 6b) is linear in the range of 0.20–1.20 mM of dopamine concentration with a correlation coefficient of determination (R^2) of 0.9938 ($n=8$). The detection limit (3σ) was 9.0×10^{-5} M.

Conclusion

The GNME successfully distinguishes the voltammetric signals of AA and DA, which are indistinguishable at the bare Au electrode. This electrode resulted in a favorable voltammetric resolution of DA and AA and the anodic potential difference (ΔE_p) was 280 mV in phosphate buffer (pH=5.00). The GNME exhibited an attractive ability to voltammetric determination of DA and AA in the same aqueous solution.

References

1. Starowicz M, Stypuła B, Ban'as J (2006) Electrochem Commun 8:227
2. Welch CM, Compton RG (2006) Anal Bioanal Chem 384:601
3. Siegel R (1993) Nano Struct Mater 3:1
4. Hayat MA (ed) (1989) Colloidal gold: principles, methods and applications, vol. 1. Academic, New York
5. Graer KC, Freeman G, Hommer MB, Natan MJ (1995) Anal Chem 67:735
6. Leibowitz FL, Zheng W, Maye MM, Zheng CJ (1999) Anal Chem 71:5076
7. Doron A, Katz E, Willner I (1995) Langmuir 11:1313
8. Shioway AN, Katz E, Willner I (2000) Chem Phys Chem 1:18
9. Brown KR, Fox AP, Natan MJ (1996) J Am Chem Soc 118:1154
10. Alivisatos AP (1996) Science 271:933
11. Zhang H, Guo Y, Wan L, Bai C (2003) Chem Commun 24:3022
12. Duron S, Rivera-Noriega R, Nkeng P, Poillerat G, Solorza-Feria O (2004) J Electroanal Chem 566:281
13. Dickinson AJ, Carrette LPL, Collins JA, Friedrich KA, Stimming U (2002) Electrochim Acta 47:3733
14. Pronkin SN, Tsirlina GA, Petrii OA, Vassiliev SY (2001) Electrochim Acta 46:2343
15. Liu Z, Lee JY, Han M, Chen W, Gan LM (2002) J Mater Chem 12:2453
16. Zhou N, Wang J, Chen T, Yu ZG, Li GX (2006) Anal Chem 78:5227
17. Liu YC, Yu CC, Yang KH (2006) Electrochem Commun 8:1163
18. Crespilho FN, Emilia Ghica M, Florescu M, Nart FC, Oliveira ON Jr, Brett CMA (2006) Electrochem Commun 8:1665
19. Agui L, Manso J, Yanez-Sedeno P, Pingarron JM (2006) Sens Actuat B 113:272
20. Yang YH, Wang ZJ, Yang MH, Guo MM, Wu ZY, Shen GL, Yu RQ (2006) Sensor Actuat B 114:1
21. Xu YY, Bian C, Chen SF, Xia SH (2006) Anal Chim Acta 561:48
22. Fu Y, Yuan R, Xu L, Chai YQ, Zhong X, Tang DP (2005) Biochem Eng J 23:37
23. Zhong X, Yuan R, Chai YQ, Liu Y, Dai JY, Tang DP (2005) Sensor Actuat B 104:191
24. Xian YZ, Wang HT, Zhou YY, Pan DM, Liu F, Jin LT (2004) Electrochem Commun 6:1270
25. Brown R, Fox AP, Natan MJ (1996) J Am Chem Soc 118:1154
26. Stamford JA, Justice JB (1996) Anal Chem 63:359A
27. Demenech A, Garcia H, Demenech-Carbo MT, Galletero MS (2002) Anal Chem 74:562
28. O'Neill RD (1994) Analyst 119:767
29. Martin DW Jr (1983) In: Martin DW Jr, Mayes PA, Rodwell VW (eds). Harper's review of biochemistry, 19th ed. Lange, Los Altos, CA
30. Koshiishi J, Imanari T (1997) Anal Chem 69:216
31. Wang P, Li Y, Huang X, Wang L (2007) Talanta 73:431
32. Zen JM, Hsu CT, Hsu YL, Sue JW, Conte ED (2004) Anal Chem 76:4251
33. Balamurugan A, Chen SM (2007) Anal Chim Acta 596:92
34. Shakkthivel P, Chen SM (2007) Biosens Bioelec 22:1680
35. Raoof JB, Ojani R, Beitollahi H (2006) Electroanalysis 18:1193
36. Raoof JB, Ojani R, Salmani-Afagh P (2004) J Electroanal Chem 57:1
37. Raoof JB, Ojani R, Rashid-Nadimi S (2005) Electrochim Acta 50:4694
38. Lei CX, Gong FC, Shen GL, Yu RQ (2003) Sens Actuat B 96:582
39. Brown KR, Walter DG, Natan MJ (2000) Chem Mate 12:306
40. Raj CR, Okajima T, Ohsaka T (2003) J Electroanal Chem 543:127
41. Lin L, Chen J, Yao H, Chen Y, Zhang Y, Lin X (2008) Bioelectrochem 73:11
42. Kumar SA, Lo PH, Chen M (2008) Biosensors and Bioelectronics 24:518
43. Raoof JB, Ojani R, Kiani A (2001) J Electroanal Chem 51:45